Excitation energies and Stokes shifts from a restricted open-shell Kohn-Sham approach

Excitation energies and Stokes shifts from a restricted open-shell Kohn-Sham approach

Tim Kowalczyk, Takashi Tsuchimochi, Po-Ta Chen, Laken Top, and Troy Van Voorhis

Citation: The Journal of Chemical Physics **138**, 164101 (2013); doi: 10.1063/1.4801790
View online: http://dx.doi.org/10.1063/1.4801790
View Table of Contents: http://scitation.aip.org/content/aip/journal/jcp/138/16?ver=pdfcov
Published by the AIP Publishing

Excitation energies and Stokes shifts from a restricted open-shell Kohn-Sham approach

Tim Kowalczyk,[a] Takashi Tsuchimochi, Po-Ta Chen,[b] Laken Top, and Troy Van Voorhis
Department of Chemistry, Massachusetts Institute of Technology, Cambridge, Massachusetts 02139, USA

(Received 22 January 2013; accepted 29 March 2013; published online 22 April 2013)

Restricted open-shell Kohn-Sham (ROKS) theory provides a powerful computational tool for calculating singlet excited state energies and dynamics. However, the possibility of multiple solutions to the ROKS equations — with the associated difficulty of automatically selecting the physically meaningful solution — limits its usefulness for intensive applications such as long-time Born-Oppenheimer molecular dynamics. We present an implementation of ROKS for excited states which prescribes the physically correct solution from an overlap criterion and guarantees that this solution is stationary, allowing for straightforward evaluation of nuclear gradients. The method is used to benchmark ROKS for vertical excitation energies of small and large organic dyes and for the calculation of Stokes shifts. With common density functional approximations, ROKS vertical excitation energies, and Stokes shifts show similar accuracy to those from time-dependent density functional theory and Δ-self-consistent-field approaches. Advantages of the ROKS approach for excited state structure and molecular dynamics are discussed. © *2013 AIP Publishing LLC*. [http://dx.doi.org/10.1063/1.4801790]

I. INTRODUCTION

Accurate methods for modeling electronically excited states in complex environments are playing an increasingly active role in the design of advanced materials, from organic semiconductors and next-generation dyes to artificial enzymes.[1,2] Several techniques rooted in density functional theory (DFT) already enjoy wide use for these excited state simulations: useful strategies include not only linear response time-dependent DFT (TDDFT),[3] but also constrained DFT,[4] Δ self-consistent-field DFT (ΔSCF-DFT),[5] and constricted variational DFT (CV-DFT),[6–8] among others.

Each of these excited state extensions of DFT possesses its own set of strengths and weaknesses. Linear response TDDFT and CV-DFT, for example, share the advantage of treating several excited states in a single calculation. The ΔSCF-DFT approach, on the other hand, offers certain practical advantages such as readily available gradients and Hessians. Despite the dominance of TDDFT in computational studies involving excited states, ΔSCF-DFT is a similarly reliable predictor of excitation energies in organic chromophores.[9] Still, the ΔSCF-DFT approach (abbreviated hereafter to ΔSCF) possesses drawbacks limiting its utility.

First, ΔSCF produces a broken-symmetry state, so the calculation of singlet excited states requires the use of a spin purification procedure.[5] Hence two independent SCF calculations must be carried out for every computed excitation energy. The second, and perhaps more severe, difficulty is that the ΔSCF orbital relaxation procedure is prone to "variational collapse," in which the SCF convergence procedure for an excited state returns to the ground state determinant. Within wavefunction-based approaches, it is possible to variationally optimize the open-shell singlet state through nonorthogonal SCF[10] or multireference schemes.[11,12] However, in solving the standard Hartree-Fock or Kohn-Sham equations, higher-energy solutions can only be obtained if variational collapse is somehow avoided. Collapse is often instigated by changes in the relative energies of frontier KS orbitals during the SCF procedure; the maximum overlap method (MOM)[13,14] is designed to address this issue by occupying orbitals at each SCF step in order of their overlap with the span of the KS orbitals from the previous SCF step. Nevertheless, neither a non-Aufbau rule nor a maximum overlap rule for orbital occupation can guarantee SCF convergence to the target state. This state of affairs makes ΔSCF less appealing for the potential energy scans and molecular dynamics simulations for which it is otherwise computationally well-suited, because the necessary convergence strategy may vary unpredictably from one geometry to the next.

Both of these shortcomings of ΔSCF can be avoided, in principle, if the spin adaption takes place at the level of the KS orbital optimization, in lieu of a *post facto* energy correction (Figure 1). The restricted open-shell Kohn-Sham (ROKS) approach to excited states,[15–17] summarized in Sec. II, offers a straightforward means of optimizing the KS orbitals to minimize any linear combination of single-determinant energies,[18] although we are primarily concerned with the case of the lowest singlet excited state. There exist more sophisticated techniques for obtaining static excited states in DFT while avoiding variational collapse.[19] Compared to other techniques which avoid variational collapse, such as CV-DFT, the relative simplicity of ROKS makes it appealing for computationally demanding applications.

[a]Present address: Department of Chemistry, Nagoya University, Nagoya, Japan.
[b]Present address: Department of Physics, National Taiwan University, Taipei, Taiwan.

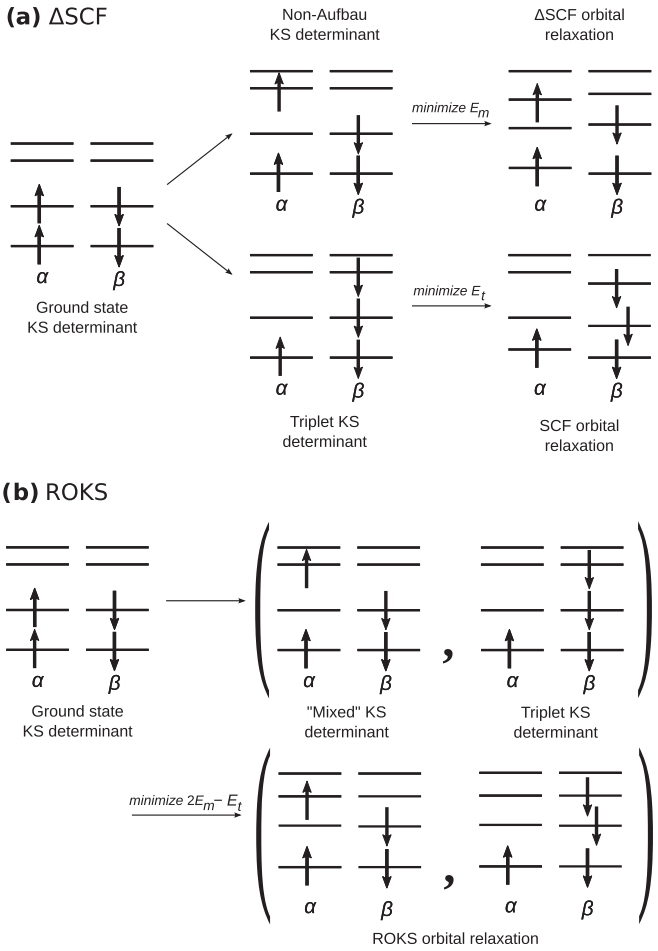

FIG. 1. Relaxation of Kohn-Sham orbitals (a) in ΔSCF, and (b) in ROKS. Note that the converged mixed and triplet determinants in ΔSCF are constructed from different KS orbitals, whereas in ROKS both determinants are built from a common set of orbitals. Furthermore, the α and β orbital sets are identical in ROKS.

Despite more than a decade of quantum chemical modeling with ROKS, both practical and fundamental questions about this strategy linger. The majority of ROKS studies have involved codes that use a plane-wave basis,[20–23] thereby precluding a thorough assessment of the performance of ROKS with hybrid XC functionals and with other recent advancements in XC functional design, such as range-separation.[24] On the more fundamental side, despite the clear analogy between the ΔSCF and ROKS ansatze, the working equations of the two methods are very distinct. Thus it merits investigation whether the excitation energies obtained by these two methods are in rough mutual agreement, and to what extent their results may be expected to differ. Furthermore, there exists a well-documented complication in ROKS in which rotations between the open-shell orbitals can artificially lower the energy of the S_1 state.[23,25,26] Efforts to address this concern have either accompanied a reformulation of the entire ROKS ansatz[23] or resulted in a set of possible solutions which must be tested on a case-by-case basis.[27] In this investigation, we determine a simple, robust resolution to the open-shell mixing problem in ROKS which ensures that the calculated electronic state is both variational and corresponds physically to the excited state of interest.

After a brief review of established ROKS theory, we present a single set of ROKS equations derived from the general SCF conditions of Hirao and Nakatsuji.[28] We also discuss the issue of indeterminacy of the ROKS equations for open-shell singlets with respect to mixing between the two open-shell orbitals, as well as the derivation of the energy gradient. After outlining computational details, we analyze ROKS vertical excitation energies for a set of small organic dyes as well as for the larger set of chromophores studied in Ref. 9. We then compare the performance of ROKS, ΔSCF, and TDDFT for the prediction of Stokes shifts using a third set of organic molecules with experimentally known Stokes shifts in the gas phase. ROKS shows promisingly good performance for both excitation energies and Stokes shifts. Finally, we conclude with our perspective on the practical utility of ROKS for excited state simulations, as well as some targets for future work.

II. THEORY

Our implementation of ROKS closely follows the formulation due to Filatov and Shaik,[15] which is itself rooted in Roothaan's vector-coupling approach to restricted open-shell Hartree-Fock theory.[29] For simplicity, we specialize immediately to the case of singlet excited states constructed from two determinants. In this formulation, the energy of a two-determinantal singlet excited state is given by the sum rule

$$E_s^{\mathrm{ROKS}} = 2E_m\left[\{\phi_i\}\right] - E_t\left[\{\phi_i\}\right], \tag{1}$$

where s, m, and t denote the singlet excited state, mixed-spin determinant, and triplet determinant, respectively, as illustrated in Figure 1. This energy expression bears similarity to the expression used for singlet excited states in ΔSCF,[5] with the key distinction that in ROKS the mixed- and triplet-state determinants are constructed from the *same set of orbitals* $\{\phi\}$, while in ΔSCF the orbitals are separately optimized for each determinant,

$$E_s^{\Delta\mathrm{SCF}} = 2E_m\left[\left\{\phi_i^m\right\}\right] - E_t\left[\left\{\phi_i^t\right\}\right]. \tag{2}$$

This fundamental difference in philosophy between the ΔSCF and ROKS approaches is illustrated schematically in Figure 1. Within Kohn-Sham DFT, the ΔSCF spin purification procedure only holds in an approximate sense because the triplet determinant is not exactly obtained from the mixed determinant by application of a spin raising operator. This problem is mitigated in ROKS through the use of a single set of orbitals for both determinants. Following precedent, we refer to the mixed and triplet determinants collectively as microstates involved in the ROKS energy expression.[15]

Variational minimization of the ROKS energy with respect to the KS orbitals leads to the complication of different Fock operators for each shell.[15,27] Nevertheless, through the general SCF operator technique of Hirao and Nakatsuji,[28] it is possible to derive a unified eigenvalue equation for closed- and open-shell orbitals in the molecular orbital (MO) basis:

$$\mathbf{FC} = \mathbf{C}\epsilon, \tag{3}$$

where **F**, **C**, and ϵ are the effective Fock matrix, MO coefficients, and orbital energies. **F** in Eq. (3) has a natural block structure defined by the different shells [closed (c), first open (a), second open (b), and virtual (v)], and it takes a different form in each of these blocks. In the Appendix, we show the derivation of this effective Fock matrix.

Expressed in terms of Fock matrices for different orbital spaces,

$$\mathbf{F}^c = 2\mathbf{F}^\alpha_m + 2\mathbf{F}^\beta_m - \mathbf{F}^\alpha_t - \mathbf{F}^\beta_t, \tag{4}$$

$$\mathbf{F}^a = 2\mathbf{F}^\beta_m - \mathbf{F}^\alpha_t, \tag{5}$$

$$\mathbf{F}^b = 2\mathbf{F}^\alpha_m - \mathbf{F}^\alpha_t, \tag{6}$$

the ROKS Fock matrix for the S_1 state is given by

$$\mathbf{F}^s = \begin{pmatrix} \mathbf{F^c} & \mathbf{F}^c - \mathbf{F}^a & \mathbf{F}^c - \mathbf{F}^b & \mathbf{F}^c \\ \mathbf{F}^c - \mathbf{F}^a & \mathbf{F}^a & \mathbf{F}^a - \mathbf{F}^b & \mathbf{F}^a \\ \mathbf{F}^c - \mathbf{F}^b & \mathbf{F}^a - \mathbf{F}^b & \mathbf{F}^b & \mathbf{F}^b \\ \mathbf{F}^c & \mathbf{F}^a & \mathbf{F}^b & \mathbf{F}^c \end{pmatrix}, \tag{7}$$

where the four rows (and columns) indicate, in order, closed-shell, first open shell, second open shell, and virtual orbitals. Then the SCF condition is given by

$$[\mathbf{F}^c, \mathbf{P}^c] + [\mathbf{F}^a, \mathbf{P}^a] + [\mathbf{F}^b, \mathbf{P}^b] = \mathbf{0}, \tag{8}$$

where

$$\mathbf{P}^c = \mathbf{P}^\beta_t, \tag{9}$$

$$\mathbf{P}^a = 2\mathbf{P}^\beta_m - \mathbf{P}^\beta_t, \tag{10}$$

$$\mathbf{P}^b = 2\mathbf{P}^\alpha_m - \mathbf{P}^\beta_t. \tag{11}$$

We construct the effective Fock matrix in three steps:

1. Build mixed ($\mathbf{P}^\alpha_m$,$\mathbf{P}^\beta_m$) and triplet ($\mathbf{P}^\alpha_t$,$\mathbf{P}^\beta_t$) density matrices from the unified set of KS orbitals.
2. Build Fock matrices ($\mathbf{F}^\alpha_m$,$\mathbf{F}^\beta_m$, $\mathbf{F}^\alpha_t$,$\mathbf{F}^\beta_t$) for the mixed and triplet determinants from the mixed and triplet densities.
3. Project linear combinations of the single-determinant Fock matrices in the MO basis onto the appropriate blocks to create the effective Fock matrix.

Using this effective Fock matrix, we solve Eq. (3) self-consistently using the standard machinery of quantum chemical SCF algorithms. The single-determinant energies are then determined from the converged KS orbitals and substituted into Eq. (1) to obtain the ROKS energy of the S_1 state.

A. Orbital mixing between open shells

Several authors have identified, in their ROKS calculations, a complication that arises when solving the ROKS equations for the lowest singlet excited state.[20,23,25–27] When the excited state possesses the same symmetry as the ground state, the ROKS algorithm formulated above permits mixing between the two open shell orbitals. This orbital mixing can artificially lower the energy of the excited state, typically by an amount commensurate with twice the singlet-triplet splitting,[23,26] potentially delivering an S_1 excitation energy that would actually make a better estimate for the triplet energy. This instability is not unexpected:[15] in fact, it was already established that a proper description of excited states of the same symmetry as the ground state requires a symmetry-dependent XC functional.[30–32]

We have observed similar energy lowering in some cases that we have tested. In such cases, we found that the final ROKS S_1 state is far from orthogonal to the reference ground state. Given that the ROKS state is expressed as a two-determinantal wavefunction, the overlap between these two wavefunctions can be computed as

$$\langle S_1 | S_0 \rangle = \sqrt{2} \det\left[\left(\mathbf{C}^\alpha_m \mathbf{S} \mathbf{C}_0\right)\left(\mathbf{C}^\beta_m \mathbf{S} \mathbf{C}_0\right)\right], \tag{12}$$

where $\mathbf{C}^\sigma_m$ and $\mathbf{C}_0$ are the MO coefficients of the mixed KS determinant of ROKS (see Figure 1) and the reference ground state. A large overlap means that such a ROKS state does not represent the S_1 excited state well. We find that this is mostly attributed to rotations between the two open shell orbitals a and b. In some situations, simply solving Eq. (7) significantly mixes these two orbitals to lower the energy. However, the ROKS equations can have multiple solutions, each of which satisfies Eq. (8). In cases where orbital mixing leads to a state with large ground-state overlap, we can easily find a more physical solution to the ROKS equations by applying a level shift to separate the energy levels of the open shell a and b orbitals. Although these solutions are not global minima, they are still stationary, and therefore analytical gradients are immediately available as explained in Sec. II B. This is an advantage of our implementation over the previous "localized" and "delocalized" solutions of other authors,[25–27] which can be non-stationary.

B. Gradient of the ROKS energy

Since the ROKS energy expression (Eq. (1)) is a linear combination of two energy expressions of KS-DFT, it is straightforward to derive the corresponding nuclear gradient $E^X_{\mathrm{ROKS}} = dE_{\mathrm{ROKS}}/dX$ where X is a nuclear position. That is to say, the gradient expression for ROKS *almost* takes a linear form built from gradients of mixed and triplet KS states. The nuclear gradient for each state can be evaluated in the usual way, see, for example, Ref. 33. However, it should be noted that, since we solve the ROKS equation, Eq. (8), instead of separate equations for each state, a term involving the Fock matrices and density matrices differs from the corresponding term obtained independently from each state. Consequently, the so-called energy-weighted density matrix[33] **W** is defined differently for ROKS,

$$\mathbf{W}^{\mathrm{ROKS}} = \mathbf{P}^\alpha_t\left(2\mathbf{F}^\alpha_m\mathbf{P}^\alpha_m + 2\mathbf{F}^\beta_m\mathbf{P}^\beta_m - \mathbf{F}^\alpha_t\mathbf{P}^\alpha_t - \mathbf{F}^\beta_t\mathbf{P}^\beta_t\right), \tag{13}$$

while for single-determinant KS,

$$\mathbf{W}^{\mathrm{KS}} = \mathbf{P}^\alpha\mathbf{F}^\alpha\mathbf{P}^\alpha + \mathbf{P}^\beta\mathbf{F}^\beta\mathbf{P}^\beta. \tag{14}$$

With this adjustment, the ROKS nuclear gradient E^X_{ROKS} can be computed simply by a linear combination of two different

nuclear gradients,

$$E^X_{\mathrm{ROKS}} = 2\tilde{E}^X_m - \tilde{E}^X_t, \tag{15}$$

where again $\tilde{E}^X_m$ and $\tilde{E}^X_t$ are evaluated with the energy-weighted density matrix in Eq. (13). Evaluation of other terms can be found in Refs. 34 and 35 and is available in the vast majority of quantum chemistry program packages. It should be noted that the above equation is only true if the variationally determined Fock matrix, Eq. (7), is used. If other variants of Fock matrix are used, one typically finds $\mathbf{W}^{\mathrm{ROKS}}$ non-Hermitian, and a correction is needed that explicitly requires computation of $\mathbf{C}^X$, because the resulting state is not variational with respect to $\mathbf{C}$, i.e., Eq. (8) is not satisfied.

III. COMPUTATIONAL DETAILS

The ROKS algorithm outlined above was implemented in a development version of the Q-CHEM 4.0 software package[36] for S_1 and T_1 excited states of molecules with closed-shell singlet ground states. A standard DIIS procedure was used to accelerate convergence.[37] Occasionally for the larger systems, virtual orbitals crossed into the energy domain of the open shell orbitals. To converge the orbitals in these cases, we introduced a level shift procedure[38] to force the virtual orbitals away from the open-shells energetically. The same technique was also used to separate closed-shell and open-shell orbital energies to aid convergence, as well as two open-shell orbitals when the resulting wavefunction had a large overlap with its ground state. Fortunately, these level shifts did not significantly increase the number of SCF cycles necessary to achieve convergence.

Geometries for the small-dye test set of Schreiber *et al*. at the MP2/6-31G* level were obtained directly from Ref. 39. ROPBE0 vertical excitation energies were also computed with the 6-31G* basis set. The basis set sensitivity of ROKS will be addressed in more detail in Sec. IV.

For the large-dye test set, the same B3LYP/6-31G* optimized geometries employed in Ref. 9 were used here. This basis set was used with the PBE0 functional for ROKS excited state calculations on the large-dye test set and for the calculation of Stokes shifts.

Stokes shifts were calculated from four single-point calculations without adjustment for the effects of vibronic coupling on the absorption and emission profiles. Absorption maxima were associated with the vertical excitation energy computed at the ground-state-optimized geometry, while emission maxima were calculated from the energy difference between the excited and ground states at the optimized geometry for the excited state, optimized using the same theory as was used for the excited state energy calculation.

IV. RESULTS AND DISCUSSION

A. ROKS energies of small organic dyes

First we validate our implementation of ROKS by considering vertical excitation energies of 27 small organic dyes for which low-lying excited state energies were recently benchmarked by Schreiber *et al*. with high-level wavefunction methods.[39] ROKS vertical excitation energies for the $S_0 \rightarrow S_1$ transition in each dye are collected in Table I. Note that the ordering of excited states in ROKS may differ from that of the wavefunction methods used to obtain the "best estimates" in Table I; in all cases the best estimate for the state most closely representative of the ROKS S_1 state was used.

Although other authors have suggested that different ROKS algorithms are necessary for different excitation symmetries, Table I shows that our ROKS algorithm provides reasonable vertical excitation energies regardless of the symmetry of the transition. This is very encouraging from a practical perspective, as it suggests that with this approach to ROKS, a single convergence strategy will work for any system (provided, of course, that the $S_0 \rightarrow S_1$ transition is well-described by a single-orbital excitation).

Generally, the overlap criterion described in Sec. II A is either near zero or near its maximum $1/\sqrt{2}$; in the latter case, applying the level shift (typically between 0.1 and 0.5 a.u.) returns a different state with near-zero overlap with the ground state. This effectively corrects for artificial lowering of the ROKS energy via mixing of the open shells. To illustrate how the level shift and the overlap criterion for judging the quality of the ROKS state enter into the calculation, we consider the case of cytosine. Without a level shift, ROKS predicts an $S_0 \rightarrow S_1$ vertical excitation energy of 3.98 eV, significantly below the best estimate, 4.66 eV. This ROKS state has an overlap with the ground state $\langle S_1|S_0\rangle = 0.6572$. With the level shift applied, the resulting ROKS state has an overlap with the ground state near zero ($\langle S_1|S_0\rangle = 0.0804$) and an excitation energy of 4.76 eV.

Regarding accuracy, RO-PBE0 tends to underestimate excitation energies, especially of $\pi \rightarrow \pi^*$ transitions, whereas it sometimes overestimates those of $n \rightarrow \pi^*$ transitions. This trend is weakly evident with the 6-31G* basis set but is more exaggerated for $\pi \rightarrow \pi^*$ transitions in the more complete 6-311+G* basis set: adding diffuse functions tends to lower the ROKS excitation energy for these transitions, sometimes substantially. Others have suggested that the underestimation of $\pi \rightarrow \pi^*$ excitation energies in ROKS may be largely due to the use of local density approximation (LDA) and generalized gradient approximation (GGA) functionals,[20] but our results suggest that hybrid functionals do not substantially correct this behavior. The predicted transition energies obtained with the LC-ωPBE0 functional show that this underestimation persists even with range-separation of the exchange interaction. The strong basis set dependence of the results is an often overlooked, but not especially surprising result considering the importance of diffuse functions for describing even valence excited states.

Having established that our ROKS implementation can deliver reasonable excitation energies for small chromophores, we proceed to benchmark ROKS for a set of larger organic dyes.

B. ROKS vertical excitation energies of large organic dyes

We evaluated ROKS vertical excitation energies for the collection of large dyes of Ref. 9 using a variety of XC

TABLE I. Lowest ROKS vertical excitation energy (in eV) for a collection of small organic dyes, compared with *ab initio* best-estimates.

		RO-PBE0 E_{ex}		RO-LCωPBE0 E_{ex}		
Molecule	Symmetry	6-31G*	6-311+G*	6-31G*	6-311+G*	Best estimate
Ethene	$\pi \rightarrow \pi^*$	7.68	7.14	7.78	7.27	7.80
Butadiene	$\pi \rightarrow \pi^*$	5.37	5.15	5.63	5.43	6.18
Hexatriene	$\pi \rightarrow \pi^*$	4.23	4.12	4.62	4.51	5.10
Octatetraene	$\pi \rightarrow \pi^*$	3.54	3.47	4.00	3.94	4.47
Cyclopropene	$\pi \rightarrow \pi^*$	6.75	6.24	6.83	6.34	7.06
Cyclopentadiene	$\pi \rightarrow \pi^*$	4.97	4.83	5.06	4.93	5.55
Norbornadiene	$\pi \rightarrow \pi^*$	4.99	4.76	5.11	4.89	5.34
Benzene	$\pi \rightarrow \pi^*$	6.51	6.28	6.66	6.44	5.08
Furan	$\pi \rightarrow \pi^*$	6.09	5.78	6.19	5.90	6.32
Pyrrole	$\pi \rightarrow \pi^*$	6.37	5.27	6.48	5.38	6.37
Imidazole	$\pi \rightarrow \pi^*$	6.43	5.76	6.56	5.83	6.19
Pyridine	$n \rightarrow \pi^*$	4.80	4.72	4.83	4.75	4.59
Pyrazine	$\pi \rightarrow \pi^*$	3.98	3.92	4.09	4.03	3.95
Pyrimidine	$n \rightarrow \pi^*$	4.34	4.29	4.44	4.39	4.55
Pyridazine	$n \rightarrow \pi^*$	3.63	3.58	3.67	3.62	3.78
Triazine	$n \rightarrow \pi^*$	4.64	4.62	4.75	4.68	4.60
Tetrazine	$\pi \rightarrow \pi^*$	2.22	2.21	2.33	2.31	2.24
Formaldehyde	$n \rightarrow \pi^*$	3.67	3.59	3.67	3.59	3.88
Acetone	$n \rightarrow \pi^*$	4.10	4.08	4.10	4.08	4.40
Benzoquinone	$n \rightarrow \pi^*$	2.46	2.49	2.70	2.73	2.80
Formamide	$n \rightarrow \pi^*$	5.48	6.84	5.46	5.35	5.63
Acetamide	$n \rightarrow \pi^*$	5.46	6.52	5.46	5.38	5.80
Propanamide	$n \rightarrow \pi^*$	5.51	6.50	5.50	5.41	5.72
Cytosine	$\pi \rightarrow \pi^*$	4.63	3.94	4.01	3.97	4.66
Thymine	$\pi \rightarrow \pi^*$	4.96	4.83	5.19	5.04	4.82
Uracil	$\pi \rightarrow \pi^*$	5.06	5.00	5.31	5.20	4.80
Adenine	$\pi \rightarrow \pi^*$	4.94	4.82	5.21	5.09	5.25
Mean error		− 0.22	− 0.23	− 0.05	− 0.24	
MAE		0.37	0.55	0.31	0.41	
RMSD		0.51	0.66	0.43	0.51	

functionals, many of which were also used in the previous ΔSCF benchmarking study. We also include results obtained within LDA to facilitate comparison with previous ROKS studies which have relied heavily on this functional. The Minnesota functionals M06-2X and M06-HF were excluded from this study because our current implementation of ROKS does not support kinetic energy density-dependent functionals.

Performance statistics across the large-dye test set are reported in Table II; a full tabulation of the constituent vertical excitation energies is available in the supplementary material.[40] In parallel with the ΔSCF results in Ref. 9, hybrid functionals with a modest fraction of exact exchange (about 20%) are most successful at reproducing the experimental excitation energies. In particular, ROPBE0 (RMSD = 0.31 eV) achieves approximately the same accuracy obtained with ΔPBE0 (RMSD = 0.28 eV) and with TD-PBE0 (RMSD = 0.32 eV) in our previous study.[9] Although the LC-ωPBE0 functional (RMSD = 0.47 eV) does not perform as well for ROKS as it did for ΔSCF (RMSD = 0.32 eV) or TDDFT (RMSD = 0.33 eV), we find that the simpler range-corrected GGA, LC-ωPBE, performs quite well for ROKS excitation energies on this test set (RMSD = 0.28 eV). However, note that the mean error (ME) and root-mean-square deviations (RMSD) for LC-ωPBE0 are of similar magnitude. Given the tendency, observed in the smaller organic dyes, for additional diffuse basis functions to lower the predicted excitation energy by 0.1 eV or more, we suspect that using a more complete basis set would significantly reduce both the ME

TABLE II. Mean error (ME), mean absolute error (MAE), and root-mean-square deviation (RMSD) of ROKS excitation energies from experiment for the test set of larger organic dyes (in eV). The 6-31G* basis set was used for each constituent calculation. Functionals are arranged in order of increasing degree of exact exchange.

Functional	ME	MAE	RMSD
LDA	− 0.56	0.57	0.66
BLYP	− 0.55	0.56	0.65
PBE	− 0.53	0.55	0.64
B3LYP	− 0.14	0.28	0.35
PBE0	− 0.04	0.24	0.31
BH&HLYP	0.43	0.43	0.51
LC-ωPBE	0.08	0.23	0.28
LC-ωPBE0	0.40	0.40	0.47
ωB97	0.91	0.91	0.94
ωB97-X	0.79	0.79	0.82

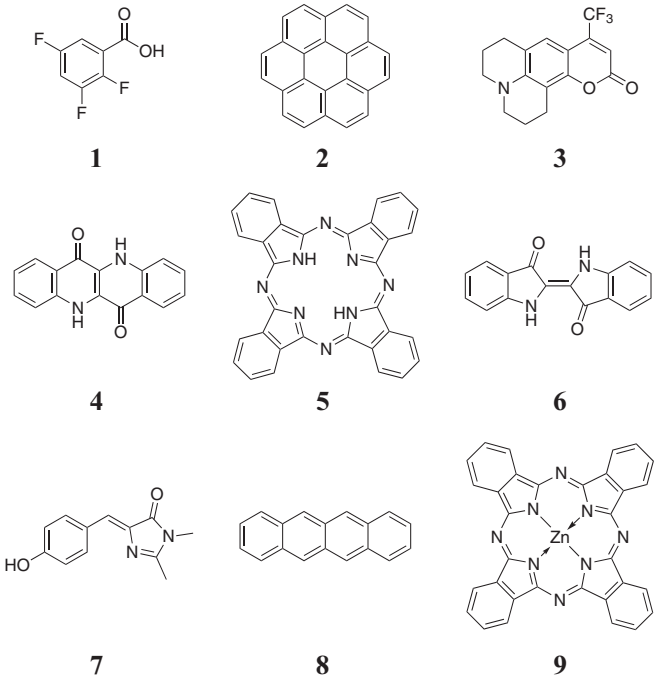

FIG. 2. Collection of organic dyes for the assessment of DFT Stokes shifts.

and RMSD of the LC-ωPBE0 excitation energies to more favorable values, while adversely affecting the performance of PBE0 to some extent.

Next we move away from ground-state equilibrium geometries and consider the application of ROKS, ΔSCF, and TDDFT to the prediction of Stokes shifts.

C. Comparison of Stokes shifts from ROKS, ΔSCF, and TDDFT

The Stokes shifts test set consists of nine chromophores for which the Stokes shift has been measured in the gas phase. Liu and co-workers presented a strategy based on the ΔSCF approach to study vertical excitation and emission in dyes, including solvatochromic effects.[41] In contrast, in preparing a set of experimental reference data, we have favored molecules with a known gas-phase Stokes shift to facilitate direct comparison between calculation and experiment. One could clearly develop a significantly larger test set if experimental results obtained in solution were to be used. However, due to the difficulties inherent in disentangling solvent effects on geometry relaxation in the excited state, we opted to study a smaller data set consisting exclusively of gas-phase experiments.

The nine chromophores are identified in Figure 2. They represent a variety of commonly encountered chromophore structures, such as an acene (**8**), a polyaromatic hydrocarbon (**2**), two phthalocyanines (**5** and **9**), and a coumarin (**3**). They also span a broad range of observed Stokes shift magnitudes, from nearly zero (free-base phthalocyanine **5**) to larger than 0.5 eV (**1** and **7**). Even larger Stokes shifts are obtainable in solution;[42] however, solvent stabilization of the excited state typically accounts for a significant fraction of the observed shift in this case.

In Table III, the calculated absorption and emission maxima are reported along with the corresponding Stokes shifts from each theoretical method and from experiment. The ground-state and ROKS excited-state optimized geometries are available in the supplementary material.[40] We find that ROKS predicts for all chromophores a Stokes shift within

TABLE III. Aborption/emission energies and Stokes shift (S.S.) of each dye in Figure 2, calculated by TDDFT, ΔSCF, and ROKS, versus experiment. All energies are in eV, and all calculations use the B3LYP functional and 6-31G* basis set. Statistics at the bottom of the table are ME, MAE, and RMSD of each method versus experiment, all in eV.

	TDDFT			ΔSCF			ROKS			Experiment
Dye	Abs.	Em.	S.S.	Abs.	Em.	S.S.	Abs.	Em.	S.S.	S.S.
1	4.33	3.81	0.52	3.41	2.45	0.95	4.35	3.79	0.56	0.52[a]
2	4.18	4.09	0.09	3.68	3.32	0.36	3.56	3.17	0.40	0.23[b]
3	3.36	2.85	0.51	3.16	2.74	0.42	3.20	2.75	0.46	0.44[c]
4	3.11	2.94	0.16	2.93	2.72	0.21	2.87	2.62	0.25	0.19[d]
5	2.07	2.01	0.05	1.93	1.81	0.12	1.83	1.69	0.14	0.02[e]
6	2.31	1.71	0.60	1.99	1.84	0.14	1.93	1.75	0.19	0.10[d]
7	3.55	2.94	0.60	3.10	2.58	0.53	3.01	2.50	0.51	0.51[f]
8	2.49	2.16	0.34	2.45	2.13	0.32	2.32	1.97	0.35	0.36[g]
9	2.09	2.03	0.07	1.91	1.81	0.10	1.85	1.73	0.12	0.12[h]
ME			0.05			0.07			0.05	
MAE			0.10			0.09			0.06	
RMSD			0.18			0.16			0.08	

[a]Reference 43.
[b]Reference 44.
[c]Reference 45.
[d]Reference 46.
[e]Reference 47.
[f]References 48 and 49.
[g]Reference 50.
[h]Reference 51.

0.2 eV of experiment, and in most cases much better, given the promising RMSDs of 0.08 eV for ROKS. The table indicates that all three methods tend to overestimate rather than underestimate the size of the Stokes shift. The pervasiveness of this trend is evident in the relatively small differences between ME and MAE, though the trend is much weaker for TDDFT. The unusually large Stokes shift predicted by ΔSCF for Dye **1** likely arises from excessive orbital relaxation, possibly due to artificial mixing with the ground state; this is evident in the underestimated absorption energy, with the problem exacerbated by geometry optimization on this state. The other outlier is the large Stokes shift predicted by TDDFT for Dye **6**, which follows from overestimation of the $S_0 \rightarrow S_1$ absorption energy.

Interestingly, the Stokes shift RMSDs are smaller than the RMSDs observed for vertical excitation energies of the large dye test set using TDDFT, ΔSCF, and ROKS. In fact, across all three theoretical methods, the predicted Stokes shifts are in agreement to within 0.1 eV for at least 6 of the 9 dyes. The same cannot be said about the absorption or emission maxima alone: consider, for example, dye **7**, for which TDDFT disagrees with ΔSCF and ROKS by more than 0.4 eV in the absorption energy. The coincidence of the predicted Stokes shifts indicates that the TDDFT, ΔSCF, and ROKS PES for these molecules, while different in absolute terms, may be more parallel than the raw energies alone would suggest.

Together, the results suggest that the ROKS approach is an effective tool for predicting the magnitude of gas phase Stokes shifts and will thus be a useful starting point for deconvoluting the roles of the environment and of dynamic effects on solution-phase Stokes shifts.

V. CONCLUSION

This study was motivated by the need for accurate, efficient excited state electronic structure methods for large, functional organic molecules in complex environments. We turned to the ROKS approach as a means of obtaining ΔSCF-like states without the specter of variational collapse; however, it has been discussed in literature that ROKS presents a different complication, the dependence of the energy on mixing between the two open shells.

We have presented and implemented an algorithm for solving the ROKS equations which satisfies the general SCF conditions of Hirao and Nakatsuji.[28] Encouragingly, and in contrast to some previous work, we find that a single convergence strategy suffices to determine the energy of the S_1 state for closed-shell molecules. We also find that the unphysical energy lowering due to orbital mixing can be avoided by use of appropriate level shift between the open shell orbitals in all cases examined. The resulting excited state has less overlap with the ground state while still being energetically stationary. The linearity of the ROKS energy expression facilitates the straightforward evaluation of gradients, which permitted us to compute excited state geometries and Stokes shifts for a test set of organic dyes.

In practice, we find that ROKS is computationally at least as efficient as ΔSCF while also avoiding the variational collapse problem. Furthermore, its accuracy is competitive with both TDDFT and ΔSCF both for energies and for geometries, as illustrated by the predicted Stokes shifts in Sec. IV.

While the present study has emphasized electronic structure, we anticipate that the favorable convergence properties of ROKS compared to ΔSCF will make ROKS a more practical tool for QM and QM/MM molecular dynamics studies. By obviating the variational collapse problem, the odds of a sudden, undetected change of electronic state from one time step to the next are significantly reduced. Furthermore, ROKS Hessians should be obtainable as a straightforward extension of the coupled-perturbed Kohn-Sham equations.[33,52] There remain important limitations to the applicability of this ROKS approach: for example, it cannot describe any arbitrary excited state, nor can it treat conical intersections in its present form. Billeter and Egli have demonstrated the calculation of nonadiabatic couplings in a modified ROKS implementation,[23] so it is likely that the challenge of treating conical intersections within our ROKS approach can be overcome. ROKS should then provide a valuable electronic structure framework for optimizing excited state reaction pathways, for which a new methodology is under investigation in our group.[53]

ACKNOWLEDGMENTS

This work was supported by a grant from the National Science Foundation (NSF) (Grant No. CHE-1058219). T.K. and L.T. thank Shane Yost and Tamar Mentzel for assistance with the curation of Stokes shift reference data. T.K. and T.T. thank Benjamin Kaduk for assistance with Q-Chem development and Jiahao Chen for fruitful discussions.

APPENDIX: GENERALIZED FOCK OPERATOR

Here we derive the ROKS effective Fock matrix for the S_1 state. By the variational principle, we obtain three Fock operators corresponding to the variation of the closed-shell orbitals (c), and the open-shell orbitals a and b:

$$\mathcal{F}^c = 2\mathcal{F}^\alpha_m + 2\mathcal{F}^\beta_m - \mathcal{F}^\alpha_t - \mathcal{F}^\beta_t, \tag{A1}$$

$$\mathcal{F}^a = 2\mathcal{F}^\beta_m - \mathcal{F}^\alpha_t, \tag{A2}$$

$$\mathcal{F}^b = 2\mathcal{F}^\alpha_m - \mathcal{F}^\alpha_t, \tag{A3}$$

where

$$\mathcal{F}^\sigma_\omega = h + 2\mathcal{J} + V^{\sigma,\omega}_{xc} \qquad (\sigma \in \alpha, \beta, \ \ \omega \in m, t). \tag{A4}$$

Here we follow the argument of Hirao and Nakatsuji[28] to derive our generalized Fock operator, $\mathcal{F}^s$. Let

$$\mathcal{R}^c = -|a\rangle\langle a|\mathcal{G}_{ai} - |b\rangle\langle b|\mathcal{G}_{bi}, \tag{A5}$$

$$\mathcal{R}^a = -\sum_i^{N_c} |i\rangle\langle i|\mathcal{G}_{ia} - |b\rangle\langle b|\mathcal{G}_{ba}, \tag{A6}$$

$$\mathcal{R}^b = -\sum_i^{N_c} |i\rangle\langle i|\mathcal{G}_{ib} - |a\rangle\langle a|\mathcal{G}_{ab}, \tag{A7}$$

where

$$\mathcal{G}_{pq} = \lambda_{pq}\mathcal{F}^p + (1-\lambda_{pq})\mathcal{F}^q, \tag{A8}$$

with λ_{pq} being nonzero real parameters. Then the SCF equations are

$$[\mathcal{F}^p + \mathcal{R}^p]|p\rangle = \varepsilon_p|p\rangle \quad \text{for } p \in c, a, b. \tag{A9}$$

Since the operator in the square brackets works only on $|p\rangle$, one can use the projection operator $|p\rangle\langle p|$. For the virtual orbitals, they remain arbitrary, and therefore we define the virtual Fock operator as

$$F^v = \sum_{pq}^{\text{vir}} |p\rangle\langle p|\mathcal{F}^c|q\rangle\langle q|. \tag{A10}$$

Then we can define our Fock operator as

$$\tilde{\mathcal{F}}^s = \sum_{p}^{all}(\mathcal{F}^p|p\rangle\langle p| + \mathcal{R}^p|p\rangle\langle p|), \tag{A11}$$

which in the matrix representation is

$$\tilde{\mathbf{F}}^s = \begin{pmatrix} \mathbf{F^c} & \lambda_{ca}(\mathbf{F}^a - \mathbf{F}^c) & \lambda_{cb}(\mathbf{F}^b - \mathbf{F}^c) & \mathbf{0} \\ \lambda_{ac}(\mathbf{F}^c - \mathbf{F}^a) & \mathbf{F}^a & \lambda_{ab}(\mathbf{F}^b - \mathbf{F}^a) & \mathbf{0} \\ \lambda_{bc}(\mathbf{F}^c - \mathbf{F}^b) & \lambda_{ba}(\mathbf{F}^a - \mathbf{F}^b) & \mathbf{F}^b & \mathbf{0} \\ \mathbf{F}^c & \mathbf{F}^a & \mathbf{F}^b & \mathbf{F}^c \end{pmatrix}. \tag{A12}$$

Note that neither the choice of the λ_{pq} nor the scaling factor in each block matters as long as they are nonzero. Therefore, we here set $\lambda_{ac} = \lambda_{bc} = \lambda_{ba} = -\lambda_{ca} = -\lambda_{cb} = -\lambda_{ab}$, and multiply each block by appropriate factors to obtain Eq. (7) after the proper Hermitization of $\tilde{\mathbf{F}}^s$.

[1] J. Hachmann, R. Olivares-Amaya, S. Atahan-Evrenk, C. Amador-Bedolla, R. S. Sanchez-Carrera, A. Gold-Parker, L. Vogt, A. M. Brockway, and A. Aspuru-Guzik, J. Phys. Chem. Lett. **2**, 2241 (2011).
[2] B. Baumeier, F. May, C. Lennartz, and D. Andrienko, J. Mater. Chem. **22**, 10971 (2012).
[3] M. E. Casida and M. Huix-Rotllant, Annu. Rev. Phys. Chem. **63**, 287 (2012).
[4] B. Kaduk, T. Kowalczyk, and T. Van Voorhis, Chem. Rev. **112**, 321 (2012).
[5] T. Ziegler, A. Rauk, and E. J. Baerends, Theor. Chim. Acta **43**, 261 (1977).
[6] T. Ziegler, M. Seth, M. Krykunov, J. Autschbach, and F. Wang, J. Chem. Phys. **130**, 154102 (2009).
[7] J. Cullen, M. Krykunov, and T. Ziegler, Chem. Phys. **391**, 11 (2011).
[8] T. Ziegler, M. Krykunov, and J. Cullen, J. Chem. Theory Comput. **7**, 2485 (2011).
[9] T. Kowalczyk, S. R. Yost, and T. Van Voorhis, J. Chem. Phys. **134**, 054128 (2011).
[10] E. R. Davidson and L. Z. Stenkamp, Int. J. Quantum Chem., Symp. **10**(S10), 21 (1976).
[11] A. Balkova and R. J. Bartlett, Chem. Phys. Lett. **193**, 364 (1992).
[12] B. O. Roos, K. Andersson, M. P. Fulscher, P. A. Malmqvist, L. SerranoAndres, K. Pierloot, and M. Merchan, Adv. Chem. Phys. **93**, 219 (1996).
[13] A. T. B. Gilbert, N. A. Besley, and P. M. W. Gill, J. Phys. Chem. A **112**, 13164 (2008).
[14] N. A. Besley, A. T. B. Gilbert, and P. M. W. Gill, J. Chem. Phys. **130**, 124308 (2009).
[15] M. Filatov and S. Shaik, Chem. Phys. Lett. **304**, 429 (1999).
[16] I. Frank, J. Hutter, D. Marx, and M. Parrinello, J. Chem. Phys. **108**, 4060 (1998).
[17] I. Okazaki, F. Sato, T. Yoshihiro, T. Ueno, and H. Kashiwagi, J. Mol. Struct.: THEOCHEM **451**, 109 (1998).
[18] M. Schulte and I. Frank, Chem. Phys. **373**, 283 (2010).
[19] V. N. Glushkov, N. I. Gidopoulos, and S. Wilson, *Frontiers in Quantum Systems in Chemistry and Physics* (Springer, 2008), pp. 451–489.
[20] S. Grimm, C. Nonnenberg, and I. Frank, J. Chem. Phys. **119**, 11574 (2003).
[21] U. F. Röhrig, I. Frank, J. Hutter, A. Laio, J. VandeVondele, and U. Rothlisberger, ChemPhysChem **4**, 1177 (2003).
[22] C. Nonnenberg, C. Bräuchle, and I. Frank, J. Chem. Phys. **122**, 014311 (2005).
[23] S. R. Billeter and D. Egli, J. Chem. Phys. **125**, 224103 (2006).
[24] J. Toulouse, F. Colonna, and A. Savin, Phys. Rev. A **70**, 062505 (2004).
[25] M. Filatov and S. Shaik, J. Chem. Phys. **110**, 116 (1999).
[26] M. Odelius, D. Laikov, and J. Hutter, J. Mol. Struct.: THEOCHEM **630**, 163 (2003).
[27] J. Friedrichs, K. Damianos, and I. Frank, Chem. Phys. **347**, 17 (2008).
[28] K. Hirao and H. Nakatsuji, J. Chem. Phys. **59**, 1457 (1973).
[29] C. Roothaan, Rev. Mod. Phys. **32**, 179 (1960).
[30] U. von Barth, Phys. Rev. A **20**, 1693 (1979).
[31] A. Görling, Phys. Rev. A **47**, 2783 (1993).
[32] M. Levy and A. Nagy, Phys. Rev. Lett. **83**, 4361 (1999).
[33] J. A. Pople, R. Krishnan, H. B. Schlegel, and J. S. Binkley, Int. J. Quantum Chem. **16**(S13), 225 (1979).
[34] P. Pulay, in *Modern Theoretical Chemistry*, edited by H. F. Schaefer III (Plenum Press, New York, 1977), Vol. 4.
[35] J. A. Pople, P. M. W. Gill, and B. G. Johnson, Chem. Phys. Lett. **199**, 557 (1992).
[36] Y. Shao, L. F. Molnar, Y. Jung, J. Kussmann, C. Ochsenfeld, S. T. Brown, A. T. B. Gilbert, L. V. Slipchenko, S. V. Levchenko, D. P. O'Neill, R. A. DiStasio, Jr., R. C. Lochan, T. Wang, G. J. O. Beran, N. A. Besley, J. M. Herbert, C. Y. Lin, T. Van Voorhis, S. H. Chien, A. Sodt, R. P. Steele, V. A. Rassolov, P. E. Maslen, P. P. Korambath, R. D. Adamson, B. Austin, J. Baker, E. F. C. Byrd, H. Dachsel, R. J. Doerksen, A. Dreuw, B. D. Dunietz, A. D. Dutoi, T. R. Furlani, S. R. Gwaltney, A. Heyden, S. Hirata, C.-P. Hsu, G. Kedziora, R. Z. Khalliulin, P. Klunzinger, A. M. Lee, M. S. Lee, W. Liang, I. Lotan, N. Nair, B. Peters, E. I. Proynov, P. A. Pieniazek, Y. M. Rhee, J. Ritchie, E. Rosta, C. D. Sherrill, A. C. Simmonett, J. E. Subotnik, H. L. Woodcock III, W. Zhang, A. T. Bell, A. K. Chakraborty, D. M. Chipman, F. J. Keil, A. Warshel, W. J. Hehre, H. F. Schaefer III, J. Kong, A. I. Krylov, P. M. W. Gill, and M. Head-Gordon, Phys. Chem. Chem. Phys. **8**, 3172 (2006).
[37] P. Pulay, Chem. Phys. Lett. **73**, 393 (1980).
[38] V. R. Saunders and I. H. Hillier, Int. J. Quantum Chem. **7**, 699 (1973).
[39] M. Schreiber, M. R. Silva-Junior, S. P. A. Sauer, and W. Thiel, J. Chem. Phys. **128**, 134110 (2008).
[40] See supplementary material at http://dx.doi.org/10.1063/1.4801790 for ROKS vertical excitation energies of the large organic dye set and for optimized ground- and excited-state geometries of the dyes in Figure 2.
[41] T. Liu, W.-G. Han, F. Himo, G. M. Ullmann, D. Bashford, A. Toutchkine, K. M. Hahn, and L. Noodleman, J. Phys. Chem. A **108**, 3545 (2004).
[42] X. Peng, F. Song, E. Lu, Y. Wang, W. Zhou, J. Fan, and Y. Gao, J. Am. Chem. Soc. **127**, 4170 (2005).
[43] T. Itoh, J. Mol. Spectrosc. **261**, 53 (2010).
[44] T. Itoh, J. Mol. Spectrosc. **252**, 115 (2008).
[45] N. P. Ernsting, M. Asimov, and F. P. Schafer, Chem. Phys. Lett. **91**, 231 (1982).
[46] G. Haucke and G. Graness, Angew. Chem., Int. Ed **34**, 67 (1995).
[47] W. Freyer, S. Mueller, and K. Teuchner, J. Photochem. Photobiol., A **163**, 231 (2004).
[48] T. M. H. Creemers, A. J. Lock, V. Subramanian, T. M. Jovin, and S. Völker, Nat. Struct. Biol. **6**, 557 (1999).
[49] Y. Ma, M. Rohlfing, and C. Molteni, J. Chem. Theory Comput. **6**, 257 (2010).
[50] R. Williams and G. J. Goldsmith, J. Chem. Phys. **39**, 2008 (1963).
[51] D. Eastwood, L. Edwards, M. Gouterman, and J. Steinfeld, J. Mol. Spectrosc. **20**, 381 (1966).
[52] A. Bèrces, R. M. Dickson, L. Fan, H. Jacobsen, D. Swerhone, and T. Ziegler, Comput. Phys. Commun. **100**, 247 (1997).
[53] L. Top, E. Hontz, A. Sinha, and T. Van Voorhis, "A novel method for generating an initial-guess reaction path: The Harmonic-Interpolated Path" (unpublished).